

Are There Common Values in First-Price Auctions? A Tail-Index Nonparametric Test

Appendix C: Additional Simulations

Jonathan B. Hill*

Dept. of Economics

University of North Carolina -Chapel Hill

Artyom Shneyerov

CIREQ, CIRANO and Concordia University, Montréal

November 27, 2011

In this appendix we replicate all simulations and the empirical study using the asymptotic variance estimator $\hat{\kappa}_{m_n}^{-2}$ for 90% confidence bands $\hat{\kappa}_{m_n}^{-1} \pm 1.64\hat{\kappa}_{m_n}^{-1}/m_n^{1/2}$ and t-statistics $m_n^{1/2}(\hat{\kappa}_{m_n}^{-1} - \kappa^{-1})/\hat{\kappa}_{m_n}^{-1}$. We also present omitted simulation figures for the cases of $L \in \{500, 1000\}$ auctions.

All simulation results verify the following: confidence bands $\hat{\kappa}_{m_n}^{-1} \pm 1.64\hat{\kappa}_{m_n}^{-1}/m_n^{1/2}$ nearly perfectly match the empirical quantiles, and the t-ratio $m_n^{1/2}(\hat{\kappa}_{m_n}^{-1} - \kappa^{-1})/\hat{\kappa}_{m_n}^{-1}$ under the null nearly universally leads to over rejection of the null by a factor of 2-3 times. In particular, by using $\hat{\kappa}_{m_n}^{-2}$ we find under PV empirical size is roughly 10%-15% for a test with nominal size 5%. By comparison if we use the kernel estimator $\hat{\sigma}_{m_n|L}^2$ empirical size is roughly 5% within a broad range of fractiles m_n . Under CV by using $\hat{\kappa}_{m_n}^{-2}$ the range of fractiles m_n for which the rejection rate is at of below 5% is roughly 1/3 to 1/2 the range obtained when using the kernel estimator $\hat{\sigma}_{m_n|L}^2$. Thus, for PV data $\hat{\sigma}_{m_n|L}^2$ consistently leads to sharp size, and for CV data $\hat{\sigma}_{m_n|L}^2$ leads for a broader window of fractiles on which empirical size is accurate (or over-rejection does not occur).

The reason for the poor performance of the test statistic $m_n^{1/2}(\hat{\kappa}_{m_n}^{-1} - \kappa^{-1})/\hat{\kappa}_{m_n}^{-1}$ can be inferred from the theory of CV and PV bids under our DGP, the simulation evidence itself, the decomposition shown in equations (29) or (33) of the main paper,

$$v_{m_n|L}^2 \sim \kappa^{-2} + \frac{n}{m_n} E \left[T_{m_n 1,l}^{(L)} T_{m_n 2,l}^{(L)} | F_L \right] \times \left\{ \frac{\sum_{l=1}^L n_l (n_l - 1)}{\sum_{l=1}^L n_l} \right\} = \kappa^{-2} + E [C_{m_n,l} | F_L],$$

and the construction of $\hat{\sigma}_{m_n|L}^2$.

Since $T_{m_n i,l}^{(L)}$ is a linear function of tail arrays the covariance $E[T_{m_n 1,l}^{(L)} T_{m_n 2,l}^{(L)} | F_L] = O_p(m_n/n) \xrightarrow{p} 0$. In small samples, however, $E[T_{m_n 1,l}^{(L)} T_{m_n 2,l}^{(L)} | F_L] \neq 0$ with positive probability [wpp] is possible. This follows since unobserved auction heterogeneity is likely to make bids positively associated

*Dept. of Economics, University of North Carolina-Chapel Hill, www.unc.edu/~jbhill, jbhill@email.unc.edu.

within the auction (Krasnokutskaya 2010). Under CV by construction bids are positively associated due to affiliation, even when there is no unobserved heterogeneity, while heterogeneity is expected to induce positive association even across PV bids in one auction. In order to understand why that may imply $E[T_{m_n 1, l}^{(L)} T_{m_n 2, l}^{(L)} | F_L] > 0$ *wpp*, notice after invoking the moment properties presented in Lemma 8 we have

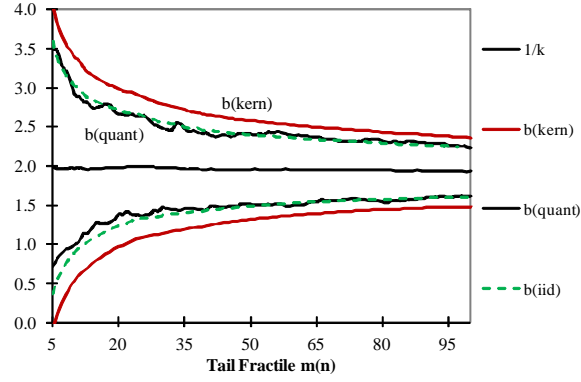
$$E \left[T_{m_n 1, l}^{(L)} T_{m_n 2, l}^{(L)} | F_L \right] \sim E \left[\left\{ (\ln (q_n / b_{1, l}^*))_+ - \kappa^{-1} I \left(b_{1, l}^* < q_n e^{u / m_n^{1/2}} \right) \right\} \left\{ (\ln (q_n / b_{2, l}^*))_+ - \kappa^{-1} I \left(b_{2, l}^* < q_n e^{u / m_n^{1/2}} \right) \right\} | F_L \right].$$

This is asymptotically mean centered since by construction $\kappa^{-1} P(b_{1, l}^* < q_n e^{u / m_n^{1/2}} | F_L) \approx (m_n / n) \kappa^{-1}$ and by Lemma 8 $E[(\ln(q_n / b_{1, l}^*))_+ | F_L] \approx (m_n / n) \kappa^{-1}$. Thus $E[T_{m_n 1, l}^{(L)} T_{m_n 2, l}^{(L)} | F_L] > 0$ *wpp* with respect to a draw of positive auction sizes $\{n_l : n_l \geq 1\}$ *if and only if* normalized bids $b_{1, l}^*$ and $b_{2, l}^*$ in auction l tend to cluster: predominantly any two bids $b_{1, l}^*, b_{2, l}^* < q_n e^{-1/\kappa}$ or $b_{1, l}^*, b_{2, l}^* \geq q_n e^{-1/\kappa}$. Since $q_n \rightarrow 0$ this implies bids tend either to cluster near the reserve price, or away from it, hence they are positively associated. Therefore positive association in CV bids in general, and PV bids with unobserved heterogeneity, may align with $E[T_{m_n 1, l}^{(L)} T_{m_n 2, l}^{(L)} | F_L] > 0$.

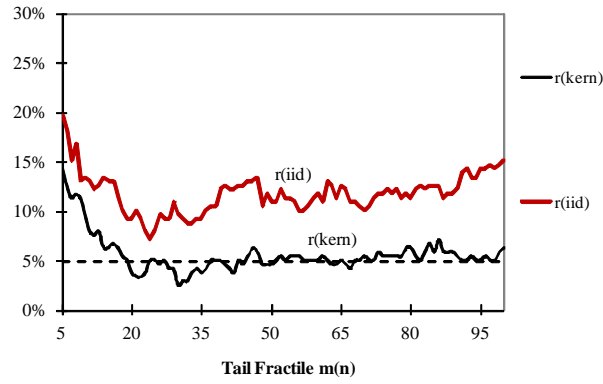
If $E[T_{m_n 1, l}^{(L)} T_{m_n 2, l}^{(L)} | F_L] > 0$ *wpp* holds then in general $v_{m_n | L}^2 > \kappa^{-2}$ in small samples. This in turn implies using $\hat{\kappa}_{m_n}^{-2}$ to estimate $v_{m_n | L}^2$ can lead to systematic under-valuation of the true small sample mean-squared-error and therefore over-rejection of our test. Our simulation evidence strongly supports this. Confidence bands computed with $\hat{\kappa}_{m_n}^{-2}$ are tighter than those with $\hat{\sigma}_{m_n | L}^2$ because in general $\hat{\kappa}_{m_n}^{-2} < \hat{\sigma}_{m_n | L}^2$, while use of $\hat{\kappa}_{m_n}^{-2}$ leads to non-negligible over-rejection of either null hypothesis. This suggests the sample version of $E[T_{m_n 1, l}^{(L)} T_{m_n 2, l}^{(L)} | F_L]$ that is implicitly computed within $\hat{\sigma}_{m_n | L}^2$ is positive *wpp*. Considering use of $\hat{\sigma}_{m_n | L}^2$ leads to a substantial improvement in sharpness of our test statistic, employing an estimator that is robust to dependence in small samples is preferred for first price auction data, in particular with unobserved heterogeneity.

Nevertheless, either test results in the same conclusion when applied to Canadian timber auctions: there is overwhelming evidence in favor of a CV strategy, and no evidence by any measure for a PV strategy.

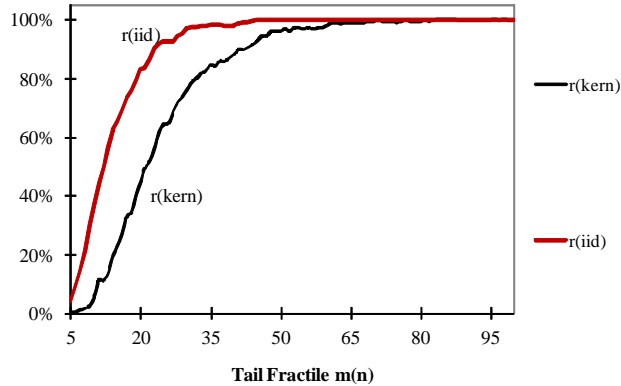
Figure C.1 : Simulated PV Data ($L = 250$)



(a) The tail index estimator $\hat{\kappa}_{m_n}^{-1}$. $b(\cdot)$ denotes the asymptotic 90% confidence band based on the variance estimator $\hat{\sigma}_{m_n}^2$ (kern), the variance estimator $\hat{\kappa}_{m_n}^{-2}$ (iid), or the sample quantiles (quant).

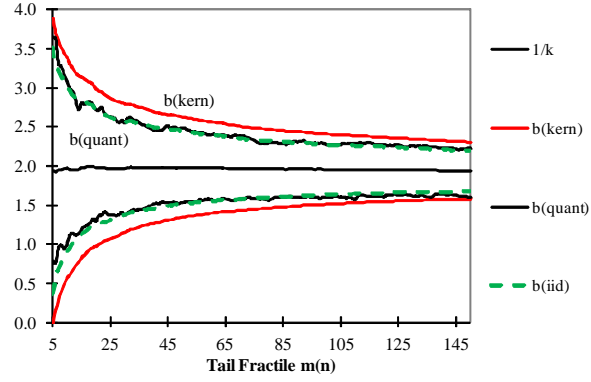


(b) The rejection frequencies: $H_0 : \text{PV } \kappa = 1/2$ against $\kappa > 1/2$. $r(\cdot)$ is the rejection frequency of the null of PV at the 5% level.

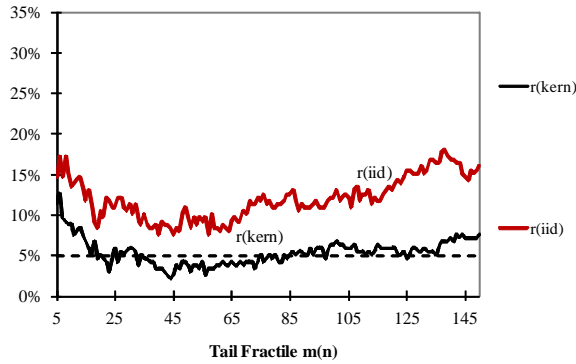


(c) The rejection frequencies: $H_0 : \text{CV } \kappa = 1$ against $\kappa < 1$. $r(\cdot)$ is the rejection frequency of the null of CV at the 5% level.

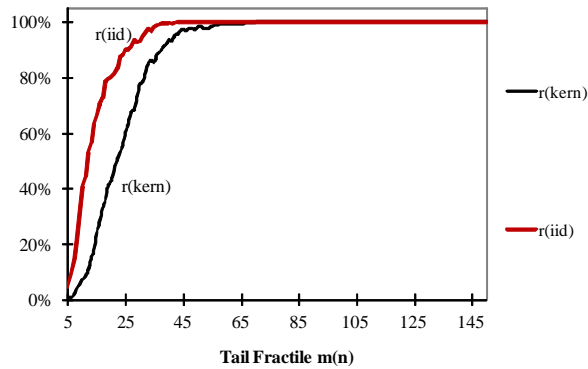
Figure C.2 : Simulated PV Data ($L = 500$)



(a) The tail index estimator $\hat{\kappa}_{m_n}^{-1}$. $b(\cdot)$ denotes the asymptotic 90% confidence band based on the variance estimator $\hat{\sigma}_{m_n}^2$ (kern), the variance estimator $\hat{\kappa}_{m_n}^{-2}$ (iid), or the sample quantiles (quant).

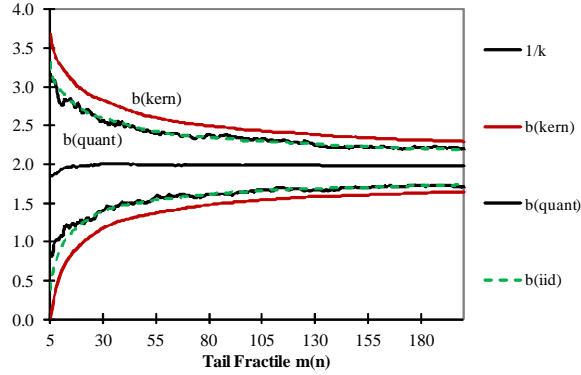


(b) The rejection frequencies: $H_0 : \text{PV } \kappa = 1/2$ against $\kappa > 1/2$. $r(\cdot)$ is the rejection frequency of the null of PV at the 5% level.

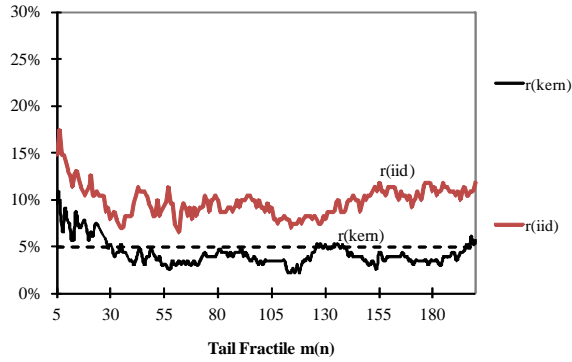


(c) The rejection frequencies: $H_0 : \text{CV } \kappa = 1$ against $\kappa < 1$. $r(\cdot)$ is the rejection frequency of the null of CV at the 5% level.

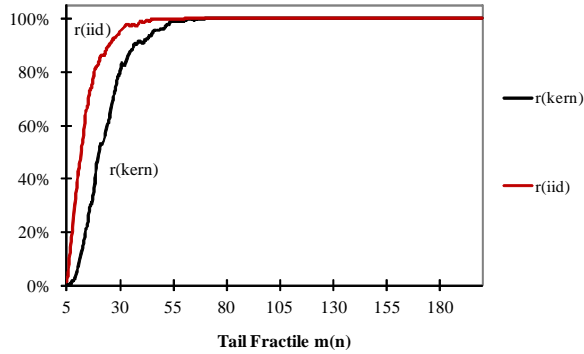
Figure C.3 : Simulated PV Data (L = 1000)



(a) The tail index estimator $\hat{\kappa}_{m_n}^{-1}$. $b(\cdot)$ denotes the asymptotic 90% confidence band based on the variance estimator $\hat{\sigma}_{m_n}^2$ (kern), the variance estimator $\hat{\kappa}_{m_n}^{-2}$ (iid), or the sample quantiles (quant).

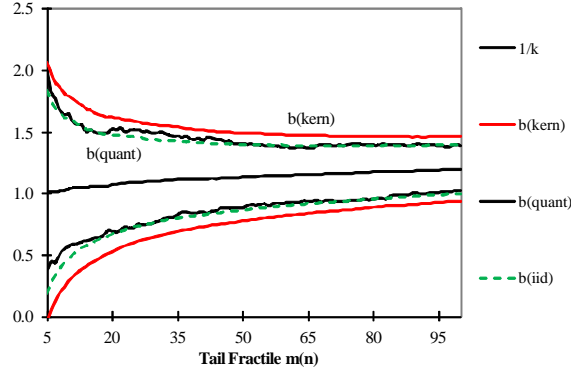


(b) The rejection frequencies: $H_0 : PV \kappa = 1/2$ against $\kappa > 1/2$. $r(\cdot)$ is the rejection frequency of the null of PV at the 5% level.

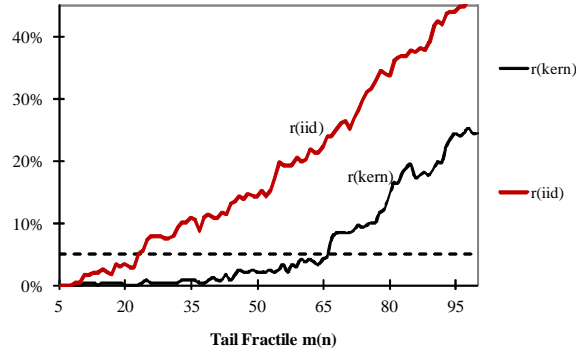


(c) The rejection frequencies: $H_0 : CV \kappa = 1$ against $\kappa < 1$. $r(\cdot)$ is the rejection frequency of the null of CV at the 5% level.

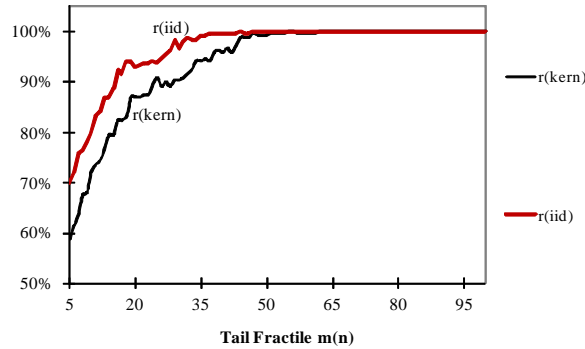
Figure C.4 : Simulated CV Data ($L = 250$)



(a) The tail index estimator $\hat{\kappa}_{m_n}^{-1}$. $b(\cdot)$ denotes the asymptotic 90% confidence band based on the variance estimator $\hat{\sigma}_{m_n}^2$ (kern), the variance estimator $\hat{\kappa}_{m_n}^{-2}$ (iid), or the sample quantiles (quant).

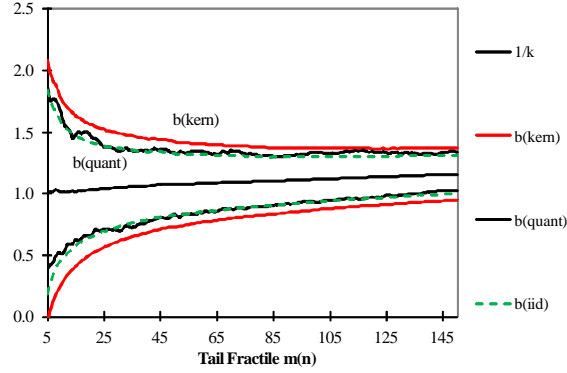


(b) The rejection frequencies: $H_0 : \text{CV } \kappa = 1$ against $\kappa < 1$. $r(\cdot)$ is the rejection frequency of the null of CV at the 5% level.

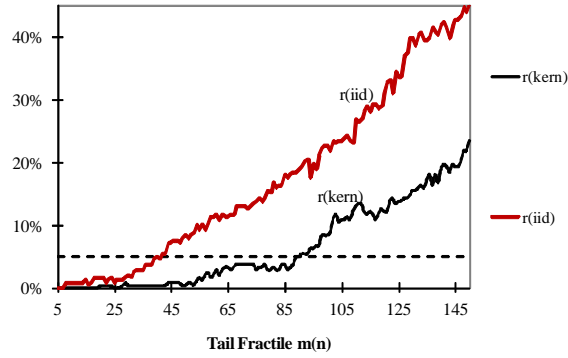


(c) The rejection frequencies: $H_0 : \text{PV } \kappa = 1/2$ against $\kappa > 1/2$. $r(\cdot)$ is the rejection frequency of the null of PV at the 5% level.

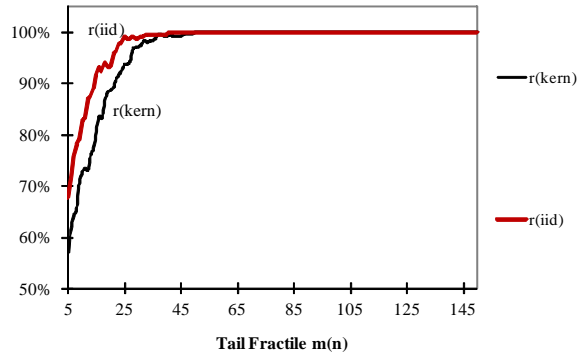
Figure C.5 : Simulated CV Data ($L = 500$)



(a) The tail index estimator $\hat{\kappa}_{m_n}^{-1}$. $b(\cdot)$ denotes the asymptotic 90% confidence band based on the variance estimator $\hat{\sigma}_{m_n}^2$ (kern), the variance estimator $\hat{\kappa}_{m_n}^{-2}$ (iid), or the sample quantiles (quant).

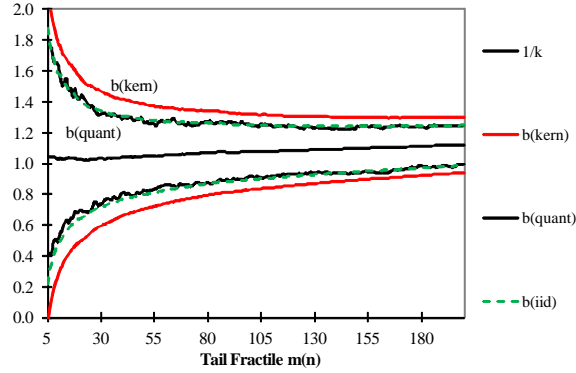


(b) The rejection frequencies: $H_0 : CV \kappa = 1$ against $\kappa < 1$. $r(\cdot)$ is the rejection frequency of the null of CV at the 5% level.

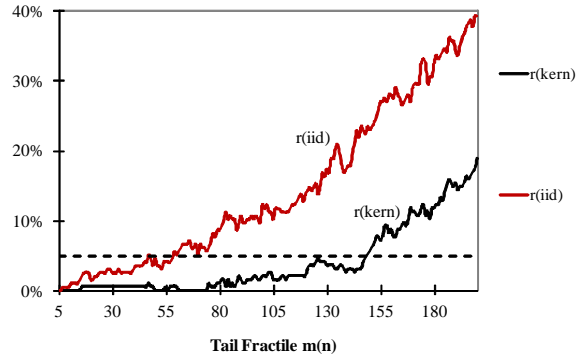


(c) The rejection frequencies: $H_0 : PV \kappa = 1/2$ against $\kappa > 1/2$. $r(\cdot)$ is the rejection frequency of the null of PV at the 5% level.

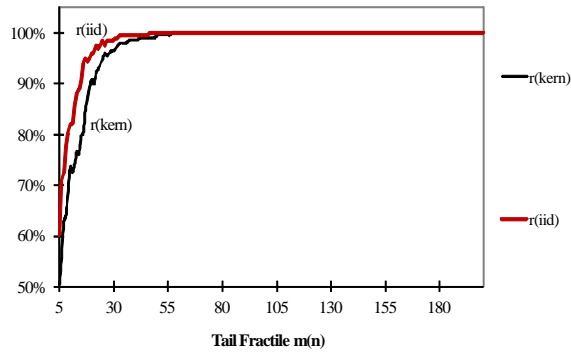
Figure C.6 : Simulated CV Data (L = 1000)



(a) The tail index estimator $\hat{\kappa}_{m_n}^{-1}$. $b(\cdot)$ denotes the asymptotic 90% confidence band based on the variance estimator $\hat{\sigma}_{m_n}^2$ (kern), the variance estimator $\hat{\kappa}_{m_n}^{-2}$ (iid), or the sample quantiles (quant).

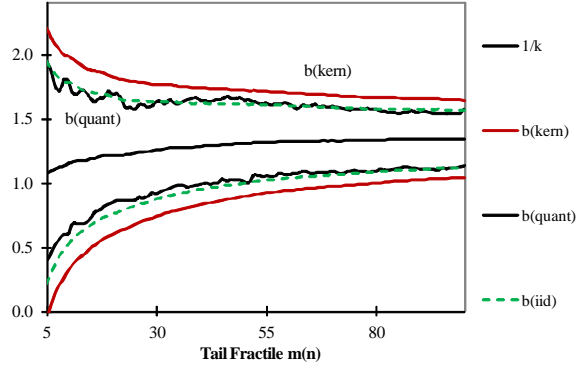


(b) The rejection frequencies: H_0 : CV $\kappa = 1$ against $\kappa < 1$. $r(\cdot)$ is the rejection frequency of the null of CV at the 5% level.

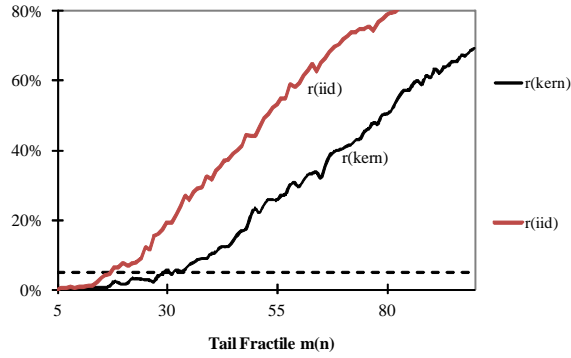


(c) The rejection frequencies: H_0 : PV $\kappa = 1/2$ against $\kappa > 1/2$. $r(\cdot)$ is the rejection frequency of the null of PV at the 5% level.

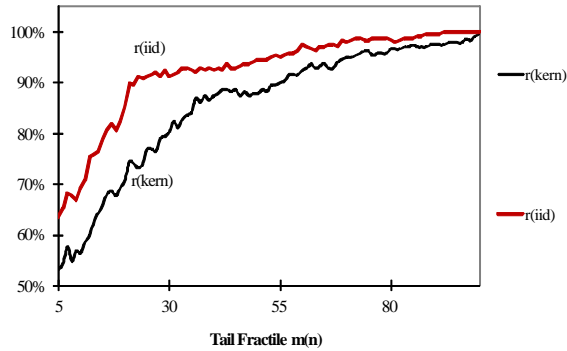
Figure C.7 : Simulated CV Data under Asymmetry (L = 250)



(a) The tail index estimator $\hat{\kappa}_{m_n}^{-1}$. $b(\cdot)$ denotes the asymptotic 90% confidence band based on the variance estimator $\hat{\sigma}_{m_n}^2$ (kern), the variance estimator $\hat{\kappa}_{m_n}^{-2}$ (iid), or the sample quantiles (quant).

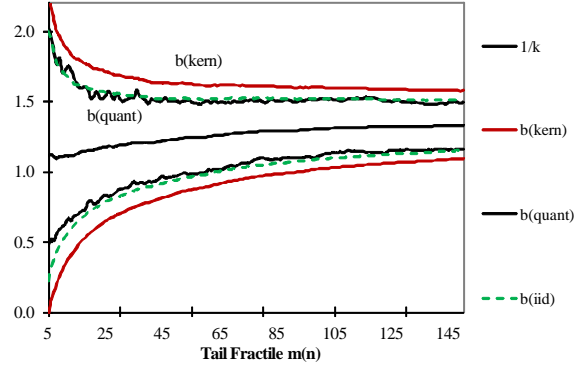


(b) The rejection frequencies: $H_0 : CV \kappa = 1$ against $\kappa < 1$. $r(\cdot)$ is the rejection frequency of the null of CV at the 5% level.

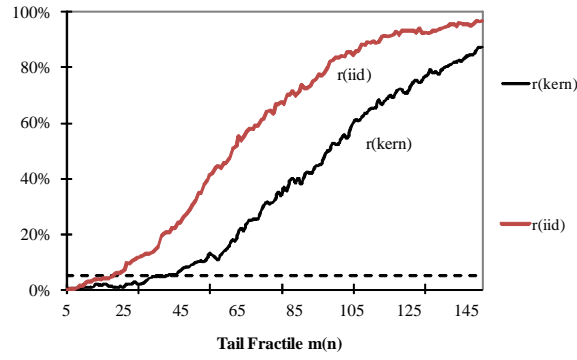


(c) The rejection frequencies: $H_0 : PV \kappa = 1/2$ against $\kappa > 1/2$. $r(\cdot)$ is the rejection frequency of the null of PV at the 5% level.

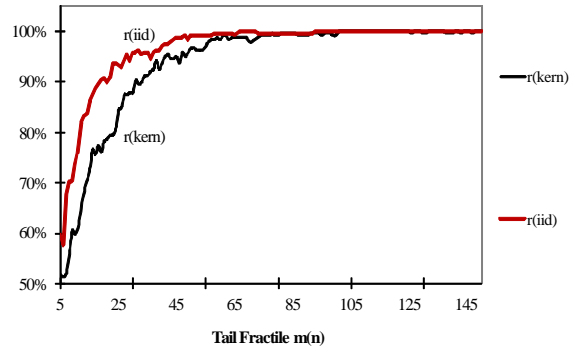
Figure C.8 : Simulated CV Data under Asymmetry (L = 500)



(a) The tail index estimator $\hat{\kappa}_{m_n}^{-1}$. $b(\cdot)$ denotes the asymptotic 90% confidence band based on the variance estimator $\hat{\sigma}_{m_n}^2$ (kern), the variance estimator $\hat{\kappa}_{m_n}^{-2}$ (iid), or the sample quantiles (quant).

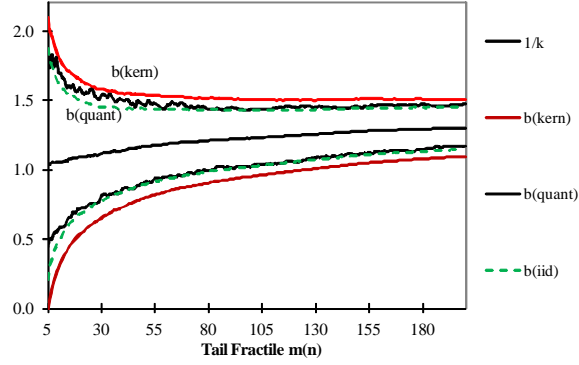


(b) The rejection frequencies: $H_0 : CV \kappa = 1$ against $\kappa < 1$. $r(\cdot)$ is the rejection frequency of the null of CV at the 5% level.

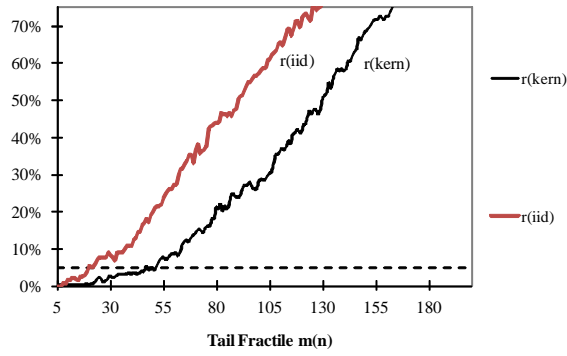


(c) The rejection frequencies: $H_0 : PV \kappa = 1/2$ against $\kappa > 1/2$. $r(\cdot)$ is the rejection frequency of the null of PV at the 5% level.

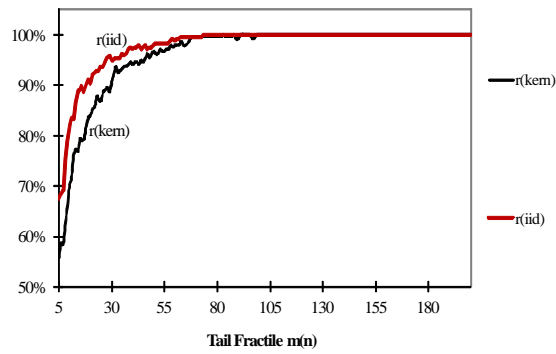
Figure C.9 : Simulated CV Data under Asymmetry (L = 1000)



(a) The tail index estimator $\hat{\kappa}_{m_n}^{-1}$. $b(\cdot)$ denotes the asymptotic 90% confidence band based on the variance estimator $\hat{\sigma}_{m_n}^2$ (kern), the variance estimator $\hat{\kappa}_{m_n}^{-2}$ (iid), or the sample quantiles (quant).

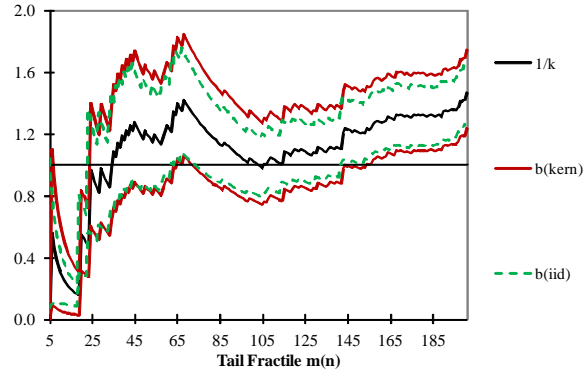


(b) The rejection frequencies: $H_0 : CV \kappa = 1$ against $\kappa < 1$. $r(\cdot)$ is the rejection frequency of the null of CV at the 5% level.

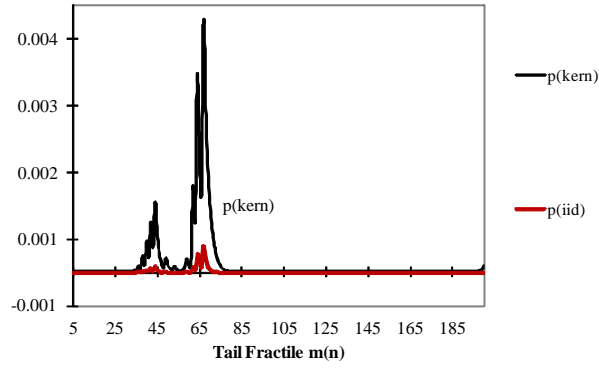


(c) The rejection frequencies: $H_0 : PV \kappa = 1/2$ against $\kappa > 1/2$. $r(\cdot)$ is the rejection frequency of the null of PV at the 5% level.

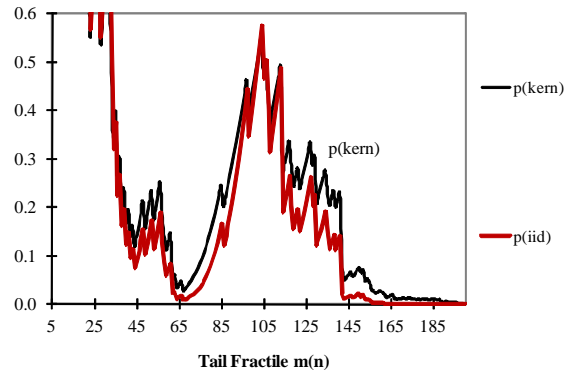
Figure C.10 : BCTS: tail index test



(a) Confidence bands $b(\cdot)$ computed from the kernel estimator $\hat{\sigma}_{m_n}^2$ (kern) and from the variance estimator $\hat{\kappa}_{m_n}^{-2}$ (iid).



(b) P-values for the t-test of $PV = 1/2$ on BCTS data.



(c) P-values for the t-test of $CV = 1$ on BCTS data.